Super strong wide TM Mie bandgaps tolerating disorders

Kiyanoush Goudarzi#1 and Moonjoo Lee#1

[1]Department of Electrical Engineering, Pohang University of Science and Technology (POSTECH), 37673 Pohang, Korea
#goudarzi@postech.ac.kr *and* moonjoo.lee@postech.ac.kr

ABSTRACT

The supplementary material proposes transmission spectra of localized modes inside the Ge-based waveguides under $\eta_r = \eta_p = 0\%$ and H-field distribution for the Ge-based B-type waveguides under $\eta_p = 20\%$ and $\eta_r = 13\%$. TE and TM Mie bandgaps in Ge and Si metamaterials under radius disordering are studied.

Localized modes

Creating straight, L-shaped, and plus shaped defects by removing dielectric rods (BK7 or Ge) localized donor modes inside the Mie and Bragg bandgaps. The defects decrease the effective refractive index of the medium; as a result, donor modes appear in the bandgaps. The donor modes come from the upper edge of the bandgaps. Transmission (T) spectra of BK7 PCs under TM polarized plane waves at $\eta_r = \eta_p = 0$, for pure lattice shows two bragg bandgaps of BG_1 and BG_2 (Fig. S1(a)), while for the Ge MMs T shows three Mie bandgap dips of TM_{01}, TM_{11}, and TM_{21} (Fig. S1(b)). The difference between the number of modes is originated from different refractive index of Ge and BK7. For the BK7 PCs of A-type straight and crossing waveguides, $T = -4$ dB at $0.79 < \frac{a}{\lambda} < 0.92$ (BG_2), while for A-type L-shaped waveguide $T = -27$ dB. The low T of the L-shaped waveguide is originated form 90° bend in the structure.

Transmission spectra under the same condition for Ge MMs for A-type of straight and crossing waveguides show $T \approx 0$ dB, and for the L-shaped waveguide $T \approx -10$ dB at $0.25 < \frac{a}{\lambda} < 0.27$ (TM_{01}). For the localized mode inside the TM_{11}, $T \approx 0$ dB at $0.37 < \frac{a}{\lambda} < 0.46$; also, for TM_{21}, T shows a variation at $0.53 < \frac{a}{\lambda} < 0.63$. The oscillations of modes in the Mie bandgaps are owning to the constructive and destructive interference of the guided waves to the structure's rods. T has the highest value over TM_{11} that is suitable to design the waveguides.

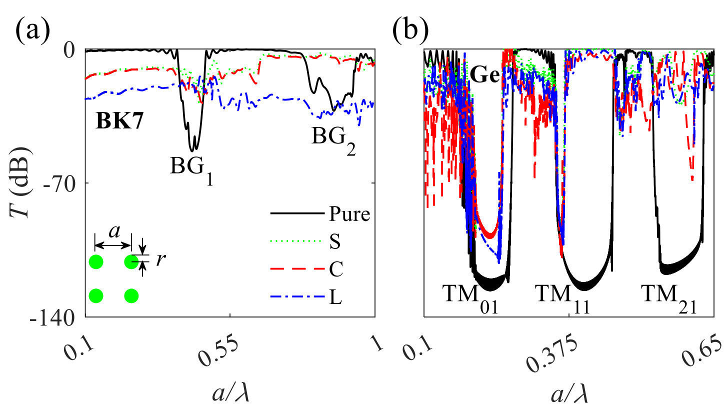

Fig. S1. (a) and (b) logarithmic transmission spectra of BK7 PCs and Ge MMs in a cubic pattern under TM polarized plane waves (H field along x direction) for pure lattice and A-type structure of straight (S), L-shaped (L), and crossing (C) waveguides at $\eta_p = \eta_r = 0\%$. For numerical calculation $r = 0.3a$.

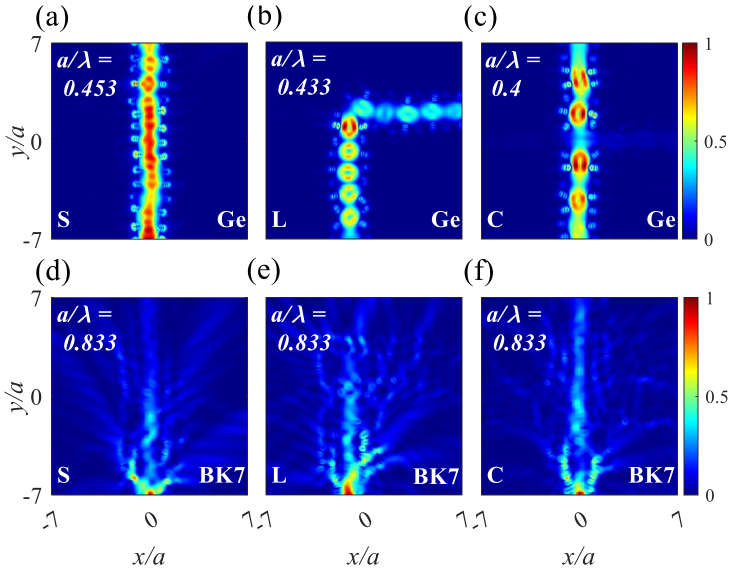

Fig. S2. (a)–(c) H-field distributions of Ge-based MMs of B-type straight (S), L-shaped (L), and crossing (C) waveguides at $\frac{a}{\lambda} = 0.453, 0.433$, and 0.4, respectively under $\eta_p = 20\%$. (d)–(f) H-field distributions of BK7-based PCs of B-type straight (S), L-shaped (L), and crossing (C) waveguides, respectively, under $\eta_p = 20\%$ at $\frac{a}{\lambda} = 0.833$.

H-field distributions

H-field distributions for the B-type waveguides contain four rows of Ge rods in air represent high coupling of incident Gaussian waves to the outputs of waveguides under $\eta_p = 20\%$ (Fig. S2(a–c)); also, show high interaction of the guided modes to the two rows which surrounded the waveguides. Owning to the position disordering, the rods in different positions induce a phase difference which results in constructive and destructive interferences in the transmitted light waves; therefore the H-field distributions have been monitored at different normalized frequencies $\frac{a}{\lambda} = 0.435, 0.433$, and 0.4 for straight, L-shaped, and crossing waveguides. As obvious from the H-filed distribution under position disordering $\eta_p = 20\%$, the sharp bend of L-shape waveguide and a horizontal line defect in plus shaped waveguide do not affect the guided modes.

H-field distributions of the B-type BK7 PCs of straight, L-shaped, and crossing waveguides at $\eta_p = 20\%$ show penetration of incident light waves over the whole structure (Fig. S2(d–f)). The sharp bend in the L-shaped waveguide and the horizontal line defect in the plus shaped waveguide affect strongly the guided modes. H-field distribution for the B-type straight, L-shaped, and crossing waveguides under radius disordering $\eta_r = 13\%$, show the high coupling of incident light waves to the outputs for Ge MMs (Fig. S3(a–c)) and very low coupling of incident light to the outputs for the BK7 PCs (S3(d–f)). For the Ge-based waveguides under radius disordering the sharp bend and horizontal line defects do not influence the guided modes while for the BK7-based wavaeguides the sharp bend and horizontal defects change the guided modes to radiation modes.

TM and TE Mie bandgaps in Ge and Si metamaterials

By decreasing the refractive index of elements in 2D all-dielectric MMs from Ge ($n = 4$) to Si ($n = 3.48$), the TE_{01} Mie bandgap mode vanishes. In comparison, by decreasing the refractive index of the elements, the TM Mie bandgaps remain which also tolerate disorderings. A Ge-based MM structure contain 15×15 elements under TE polarization incident plane waves over $0.22 < \frac{a}{\lambda} < 0.62$ reveals a weak and narrow TE_{01} bandgap with $T = -88$ dB at $0.3 < \frac{a}{\lambda} < 0.33$, and the narrow TE_{11} and weak Bragg bandgaps (BG) that do not show robustness to radius disordering (Fig. S4(a)). In contrast, the structure under illumination of TM plane wave over $0.1 < \frac{a}{\lambda} < 0.72$ demonstrates three intense-broad TM Mie bandgaps of TM_{01} ($0.17 < \frac{a}{\lambda} < 0.266$), TM_{11} ($0.351 < \frac{a}{\lambda} < 0.461$), and TM_{21} ($0.53 < \frac{a}{\lambda} < 0.63$). TM_{01} show position robustness of $\eta_r = 34\%$ with inevitable cost of band narrowing, TM_{11} represents robustness of $\eta_r = 20\%$, and TM_{21} does not show robustness to radius disordering (Fig. S4(b)).

In Si-based MMs TE_{01} approximately diminished and disappeared (Fig. S4(c)). In contrast, the Si-based structure reveals the strong and broad Mie bandgaps of TM_{01} ($0.21 < \frac{a}{\lambda} < 0.3$), TM_{11} ($0.4 < \frac{a}{\lambda} < 0.5$), and TM_{21} ($0.62 < \frac{a}{\lambda} < 0.68$), respectively, in which TM_{01} shows strong robustness to radius disordering of $\eta_r = 34\%$ (Fig. S4(d)).

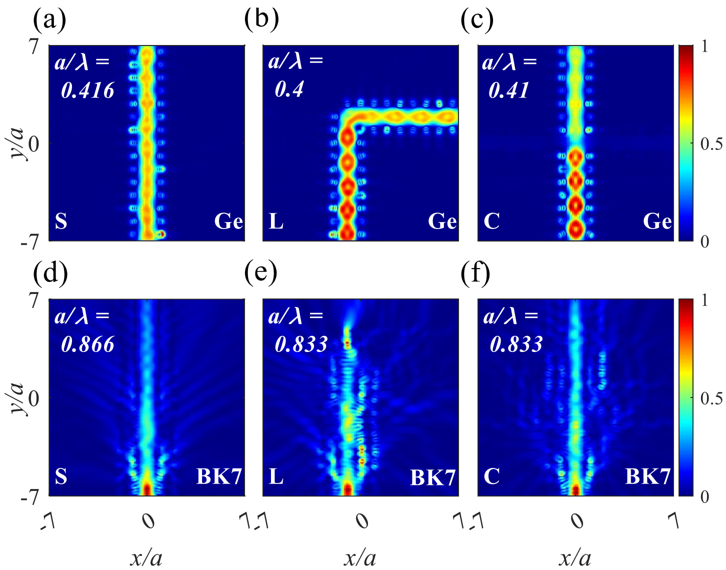

Fig. S3. (a)–(c) H-field distributions of Ge-based MMs of B-type straight (S), L-shaped (L), and crossing (C) waveguides at $\frac{a}{\lambda} = 0.416, 0.4$, and 0.41, respectively under $\eta_r = 13\%$. (d)–(f) H-field distributions of BK7-based PCs of B-type straight (S), L-shaped (L), and crossing (C) waveguides, respectively, under $\eta_r = 13\%$ at $\frac{a}{\lambda} = 0.833$.

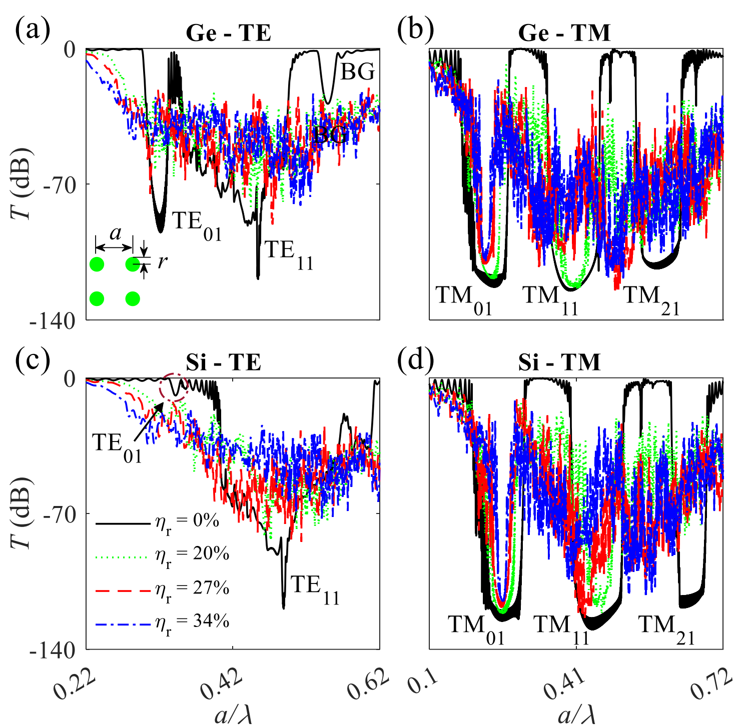

Fig. S4. Logarithmic transmission spectra of 15×15 Ge rods in air under illumination of TE (a) and TM (b) plane waves, respectively. Logarithmic transmission spectra of 15×15 Si rods in air under illumination of TE (c) and TM (d) plane waves. Solid black, dotted green, dashed red, and dot-dashed blue curves represent the position disordering of $\eta_r = 0, 20, 27$ and, 34%, respectively.